Contribution of Microwave Fourier Transform Spectroscopy to the Investigation of Nuclear Quadrupole Coupling *

Helmut Dreizler

Abteilung Chemische Physik im Institut für Physikalische Chemie
der Christian-Albrechts-Universität zu Kiel, W-2300 Kiel

Z. Naturforsch. **47a**, 342–352 (1992); received August 5, 1991

Dedicated to Prof. Dr. Yuichi Kamura, Tokyo, on occasion of his seventyfifth Birthday

By simple examples it is shown how fine structures in rotational spectra of free molecules can be used to analyse nuclear quadrupole coupling. It is demonstrated that microwave Fourier transform spectroscopy is an adequate tool for these studies. Examples for different nuclei illustrate the present possibilities.

Introduction

The objects studied by microwave (MW) spectroscopy are free dipolar molecules or molecular aggregates in a gaseous sample [1]. Typically, the pressure is 1 mTorr (0.13 Pa), the mean free path between collisions 1 cm, and the period between collisions 30 μs. That means that a molecule rotates typically $3 \cdot 10^5$ times between collisions.

In the following I will illustrate the problems by the most simple examples.

In MW spectroscopy, electric dipole transitions are observed between rotational energy levels. For linear molecules like carbonylsulfide, $^{16}O^{12}C^{32}S$, the rotational Hamiltonian H_R is most simple:

$$\hat{H}_R = B\hat{P}^2. \qquad (1)$$

Here the rotational constant is

$$B = \frac{h}{8\pi^2 I}. \qquad (2)$$

with I being the moment of inertia and $\hat{P}^2$ the squared angular momentum operator [2], the molecule being assumed to be rigid. The energy eigenvalues of (1) are

$$E_R = BJ(J+1) \qquad (3)$$

with the angular momentum quantum number $J = 0, 1, 2, \ldots$. Figure 1 shows a part of a level diagram and the corresponding spectrum. For symmetric top molecules like methyl chloride, CH_3Cl, or asymmetric tops like sulfur dichloride, SCl_2, the Hamiltonians and energy eigenvalue expressions are more complicated [3, 4].

The analysis of rotational spectra $\{\nu_i\}$ *without* additional effects leads to structural information, e.g. bond lengths and bond angles:

$$\{\nu_i\} \rightarrow B \rightarrow I \rightarrow \begin{matrix}\text{bond lengths}\\ \text{bond angles}.\end{matrix}$$

The difficulty arising from the fact that a spectrum of a linear molecule provides only one rotational constant is overcome by the investigation of a sufficient number of isotopomers [5]. The structure is assumed to be unchanged. For nonlinear symmetric and asymmetric top molecules the situation is similar. The procedure of structure determination is analogous.

MW spectroscopy is still an interesting field as additional effects modify the spectra. These modifications are observable due to the high sensitivity, resolution and precision of modern spectrometers.

Nuclear Quadrupole Coupling

One of these effects is nuclear quadrupole coupling [6]. Here the angular momentum of a nucleus is coupled to the molecular rotation by an electric quadrupole moment of the nucleus and a nonspherical electric field distribution, the electric field gradient at the

---

* An invited paper given at the XIth International Symposium on Nuclear Quadrupole Resonance, King's College, London, United Kingdom, July 15–19, 1991.

Reprint requests to Prof. Dr. H. Dreizler, Institut für Physikalische Chemie, Universität Kiel, Olshausenstraße 40, W-2300 Kiel 1, FRG.

0932-0784 / 92 / 0100-0342 $ 01.30/0. – Please order a reprint rather than making your own copy.

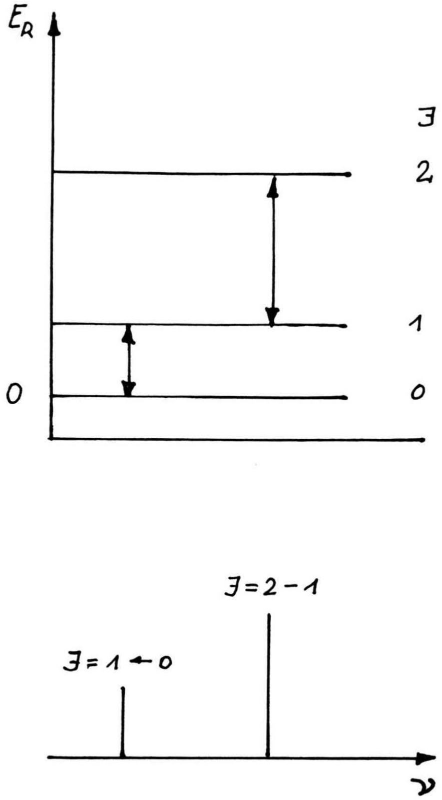

Fig. 1. Part of the rotational energy levels of a linear molecule like carbonylsulfide, $^{16}O^{12}C^{32}S$, according (3), and the corresponding rotation spectrum. J designates the angular momentum quantum number, ν the frequency.

site of the nucleus, produced by the molecular charges outside the nucleus.

The rotational Hamiltonian and the energy eigenvalues change to

$$\hat{H} = \hat{H}_R + \hat{H}_Q \quad [7]. \tag{4}$$

and

$$E = E_R + E_Q = BJ(J+1) - eQq\, Y(J, I, F) \tag{5}$$

with e elementary charge,
Q quadrupole moment,
$q = \dfrac{\partial^2 V}{\partial z^2}$ field gradient,
V electric potential,
z coordinate along the molecular axis,
$Y(J, I, F)$ Casimir function,
I nuclear spin quantum number,
F overall angular momentum quantum number.

Isocyanogen, $C^{15}NC^{14}N$ [8] is an example. Part of a schematic level scheme and spectrum is given in Figure 2.

Extraction of information from the hyperfine (hfs) splittings $\{\Delta\nu_i\}$ needs high *resolution, sensitivity* and *dynamic range* of the spectrometers. It follows the scheme (compare (5))

$$\begin{tikzcd} \{\nu_i\} \arrow[r] & B \arrow[dr] & \\ \{\Delta\nu_i\} \arrow[rr] & & eQq = eQ\dfrac{\partial^2 V}{\partial z^2}. \end{tikzcd}$$

In MW spectroscopy the product Qq of the nuclear and molecular parameters is not separabel.

For asymmetric top molecules with rotational constants A, B, and C the diagram modifies to

$$\begin{tikzcd} \{\nu_i\} \arrow[r] & A, B, C \arrow[dr] & \\ \{\Delta\nu_i\} \arrow[rr] & & \chi_{gg} = eQ\dfrac{\partial^2 V}{\partial g^2}, \quad g = a, b, c, \end{tikzcd}$$

and in favorable cases to

$$\chi_{gg'} = eQ\frac{\partial^2 V}{\partial g\, \partial g'}, \quad g, g' = a, b, c.$$

For symmetric top molecules the analysis is similar. If a molecule contains more than one quadrupole nucleus the spectra and their analysis are more complicated [10, 11]. The Hamiltonian must be extended to

$$\hat{H} = \hat{H}_R + \sum_{i=1}^{n} \hat{H}_{Qi}. \tag{6}$$

With an analysis we reached in Kiel $n = 3$ [12] with HN_3 via the analysis of $H^{15}NNN$ and $HNN^{15}N$, and the same way for CH_3N_3 [13]. The spectra are very complicated and higher resolution is desirable. The assignment will stay a problem in those cases.

Magnetic Spin-Rotation Coupling

If the MW spectra are measured with very high resolution, which will be shown below, an additional coupling between a nucleus and the molecular frame can be observed. Here the nuclear magnetic dipole moment interacts with the magnetic field produced by the rotating charge cloud of the molecule. The effects are small but noticeable.

The interaction Hamiltonian is [14]

$$\hat{H}_{SR} = -\hat{\mu}_I \cdot H \tag{7}$$

with

$$\hat{\mu}_I = g_I\, \beta_I\, \hat{I}. \tag{8}$$

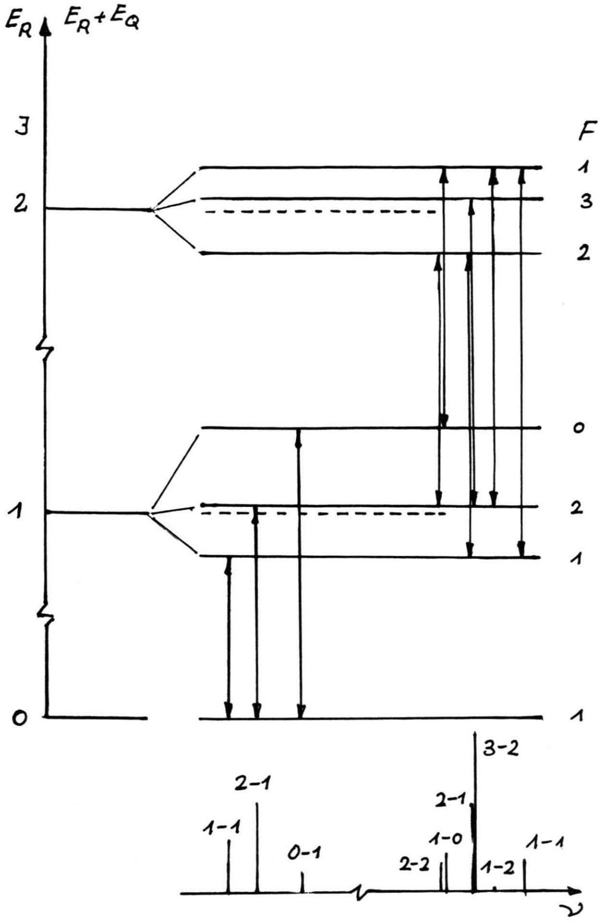

Fig. 2a. Part of the rotational energy levels of a linear molecule with one coupling nucleus like isocyanogen-^{15}N, $C^{15}NC^{14}N$. Left side without nuclear quadrupole coupling. Right side with nuclear quadrupole coupling as given by (5). Below the resulting rotational spectrum.

Here $\hat{\mu}_I$ is the magnetic dipole operator of the nucleus considered, g_I its gyromagnetic ratio, β_I the nuclear magneton, $\hat{I}$ the nuclear spin operator and H the magnetic field produced at the position of the nucleus by the rotating charge cloud of the molecule.

For example some nuclear magnetic dipole moments in units of the nuclear magneton [15] are $\mu(H)=2.79$, $\mu(^{11}B)=2.69$, $\mu(^{12}C)=0$, $\mu(^{13}C)=0.7$, $\mu(^{16}O)=0$, $\mu(F)=2.63$.

All nuclei with $I \geq 1/2$ produce this interaction. It increases with more rapid molecular rotation or with smaller moments of inertia of the molecule. For linear molecules the additional energy contribution is [16]

$$E_{SR} = C_I[F(F+1)-I(I+1)-J(J+1)]/2 \quad (9)$$

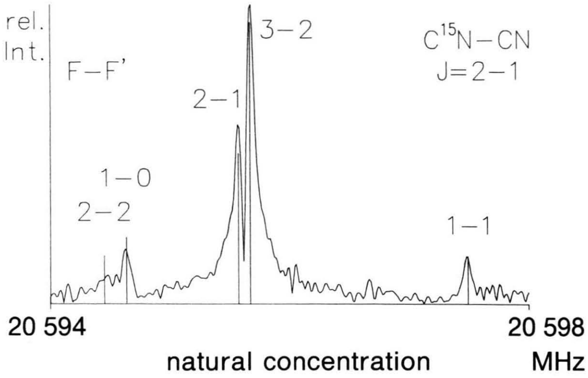

Fig. 2b. 4 MHz section of a recording of the $J=2-1$ transition of $C^{15}NC^{14}N$. Quadrupole moment of nitrogen $Q=0.02 \cdot 10^{-24}$ cm^2 [9]. F designates the total angular quantum number. Experimental conditions: ^{15}N in natural abundance, pressure 0.75 mTorr, temperature −60 °C, 20 ns sample interval, 1024 data points supplemented by 3072 zeros before Fourier transformation, 600 · 32 k measuring cycles, polarising frequency 20 592 MHz.

with C_I being the spin-rotation coupling constant typical for a given molecule. For cyanogen iodide, $IC^{15}N$ we got [17] $C_I(I)=10.02(8)$ kHz and $C_I(^{15}N)=-1.51$ kHz in comparison to $eqQ(I)=-2419.9647(25)$ MHz. Spin-rotation coupling is small but noticeable.

The influence of the spin-rotation interaction is illustrated in Fig. 3 for a rotational energy level of a molecule without and with nuclear quadrupole hyperfine structure (nqhfs).

The considerations given so far indicate that especially in the case of multiple interactions a complicated theory has to be applied with great care to analyse the spectra. All approximations must be checked. Often large Hamiltonian matrices must be diagonalized.

The analysis of the spectra may be further complicated by internal rotation, inversion, vibration and centrifugal distortion effects.

Consequences for the Experiments

With MW spectroscopy, especially Stark modulated spectroscopy [19, 20], since 1945 a large number of molecular spectra have been investigated [21]. Many coupling constants, especially of "strong" coupling nuclei like Cl, Br, and I but less of weak or intermediate coupling nuclei like D, B or N, were determined.

With the advent of MW Fourier transform (FT) spectroscopy the experimental situation improved further. The sensitivity increased roughly by a factor

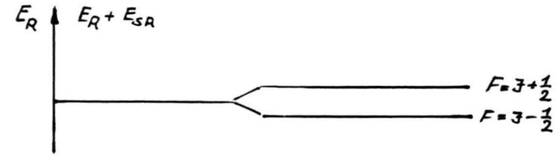

Fig. 3a. A rotational energy level with splitting by spin-rotation coupling of a single nucleus with $I=1/2$ without NQHFS.

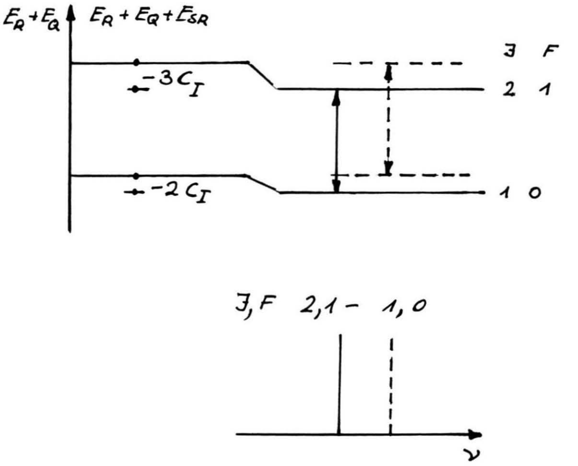

Fig. 3b. Selected rotational energy levels of hydrogen cyanide, HCN, without (left) and with (right) spin-rotation coupling, $C_I(^{14}N)=10.4(3)$ kHz [18] and resulting shift of the NQHFS, $F=1-0$ component of the $J=2-1$ transition.

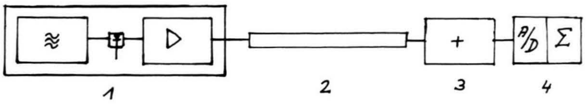

Fig. 4. Schematic set up of a waveguide MWFT spectrometer. **1** Phase stabilised high power microwave pulse source. **2** Waveguide sample cell. **3** Superheterodyne detection system. **4** Transient recorder, averager and computer.

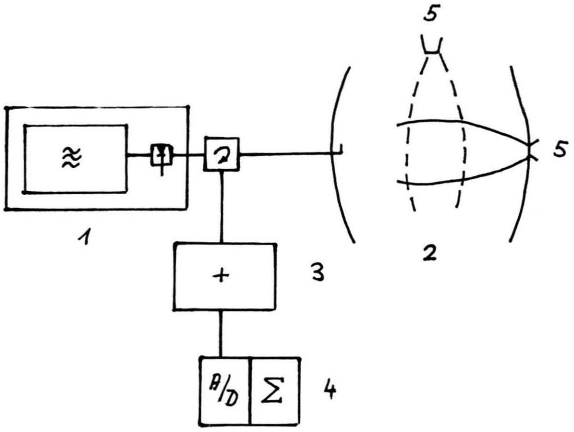

Fig. 5. Schematic set up of a pulsed molecular beam MWFT spectrometer. **1** Phase stabilised microwave pulse source. **2** Fabry Perot resonator cavity with pulsed molecular beam, for higher resolution with beam and cavity axes parallel [26]. **3** and **4** see Figure 4. **5** Beam nozzle.

of ten, the resolution in two steps with different setups roughly by a factor of hundred.

In Figs. 4 and 5, I give schematic diagrams of a waveguide MWFT spectrometer and of a pulsed beam MWFT spectrometer. Both developments were initiated by the late W. H. Flygare, Urbana, Ill. [22, 23]. Our laboratory followed with an improved waveguide MWFT spectrometer [24] shortly later. The beam instrument was recently improved in our laboratory for a scanning version [25] and a version with increased resolution [26]. For details of our spectrometers see [24, 27–44].

In the waveguide MWFT instrument a strong MW pulse between 50 to 2000 ns is produced, 1. The MW carrier frequency is phase stabilized and would have a cw-power of 1–20 watts. The MW pulse polarises the molecular ensemble in the sample cell, 2. The response of the molecules, the transient emission, is superheterodyne detected, 3, and converted to a frequency band centered at 30 MHz. The transformed transient emission is digitized with 10 ns interval for 1024 to 4096 data points, averaged up to 10^8 times and Fourier transformed, 4.

We reach an experiment repetition rate of 75 kHz when measuring 1024 data points [40]. Without the time for MW pulse application and damping the reflected MW pulse, the total time is used for measuring. The crucial instrument, a transient recorder, is not yet commercially available with sufficient specifications.

In the beam instrument (Fig. 5) a MW-pulse is formed, 1, and applied to a molecular "cloud" of a supersonic pulsed beam, 2, in a Fabry Perot cavity. A high Q cavity increases the MW power density in the sample space. The transient emission signal is superheterodyne detected, down converted, 3, digitized and averaged, 4.

As the pumping speed is limited by a reasonable size of the vacuum pumps, a repetition rate of 30 Hz is

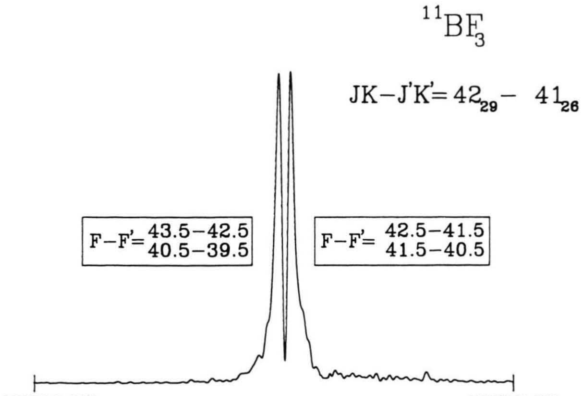

Fig. 6. Rotational transition $J_{K^-} = 42_{29}-41_{26}$ of boron trifluoride, $^{11}BF_3$, showing hfs splitting. Temperature −53 °C, pressure 4 mTorr, $3.3 \cdot 10^7$ averaging cycles, sample interval 10 ns, 1024 data points supplemented by 3072 zeros prior to Fourier transformation, spectral point distance 25 kHz, polarizing frequency 15 380.2 MHz.

possible. This rate may be increased by applying several MW pulses during the same beam shot [45]. Usually 1 to 1000 repetitions are sufficient.

In both instruments all frequencies and trigger pulse trains must be referenced to a master frequency to allow averaging.

The reason for the increased sensitivity is, that waveguide MWFT "scans" a certain spectral region simultaneously (Felgett advantage) using all the time for measuring except the time necessary for polarizing the molecular ensemble. For molecules with small dipole moments ($\mu < 0.3$ Debye), the Stark modulation is difficult to apply, especially for high J transitions. MWFT spectroscopy can produce spectra by long polarizing MW pulses. The molecules methane, CH_4, [46, 47], germane, GeH_4, [48, 49], propane, $(CH_3)_2CH_2$, [50], and borontrifluoride, $^{11}BF_3$, [51, 52], may be mentiond here, as is demonstrated in Fig. 6 for $^{11}BF_3$.

The resolution in waveguide MWFT spectroscopy is increased as the method has no modulation broadening (usually 30 or 100 kHz in Stark spectroscopy), no saturation broadening and inferior pressure broadening. It proved that it is favourable to reduce the sample pressure to 1 mTorr (0.133 Pa) or less, whereas in Stark spectroscopy 10 mTorr or more is usual.

So Doppler broadening, wall collision broadening, and residual pressure broadening often determine the line width, as is demonstrated in Figure 7.

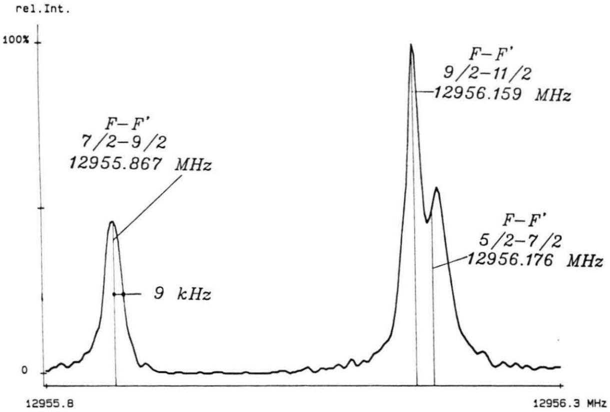

Fig. 7. A section of 500 kHz out of a power spectrum of 5 MHz length of cyanogen iodide, $IC^{14}N$, showing ^{14}N hyperfine structure of a $F_1 = 7/2-9/2$ component of the $J = 2-1$ transition. Temperature −30 °C, pressure 0.25 mTorr (0.03 Pa), $1.6 \cdot 10^6$ averaging cycles, sample interval 100 ns, 1024 data points supplemented by 3072 zeros before Fourier transformation, polarizing frequency 12 955.0 MHz. – Experimental half width at half height $\Delta\nu_{exp} = 9$ kHz, Doppler width $\Delta\nu_{Doppler} = 6$ kHz, $\Delta\nu_{wall} = 2$ kHz [64].

For beam MWFT spectroscopy the situation is slightly different. The main contribution to the increased sensitivity is the dramatic increase of the difference ΔN in occupation numbers of the involved levels by cooling to approximately 5 K. The Felgett advantage is inferior as the instrument is band limited by the use of the MW cavity. For molecules with low dipole moment the polarization is easier by low power MW sources as the high Q-value of the cavity increases the MW field strength. A disadvantage is that the repetition rate is low (30 Hz) and limited by the vacuum pump capacity.

The resolution is improved as no modulation, power and collision broadening occurs. The Doppler broadening is decreased but not completely eliminated. The transit time broadening contributes here. The broadening effects are not yet clearly understood. In Fig. 8 I give an example of the line width we reached with a beam coaxial to the cavity symmetry axis.

The determination of the transition frequency has to be made with great care because of serious overlapping effects [53, 54]. For a more detailed description of MWFT spectroscopy see [55, 56].

Experimental Results

In the following I give a selection of results for quadrupole coupling tensors. The values are in general by a factor ten more precise than those obtained

Table 1–4. Quadrupole and spin-rotation coupling constants of selected molecules containing boron, bromine, chlorine, deuterium, iodine, and nitrogen.

Table 1. Trivalent boron, ^{11}B, Spin $I=3/2$, $Q=0.04$ barn [15].

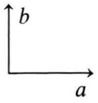	gg	$\chi_{gg}(^{11}B)$ [MHz]	$\chi_{gg}(^{14}N)$ [MHz]	[kHz]	Ref.
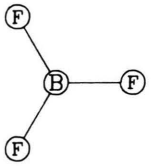	cc	3.002(13) *	–	$(C_x-C_y)(F)=8.24(23)$	[52]
	Borontrifluoride, BF_3				
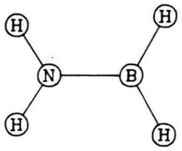	aa	$-1.684(14)$	$+0.095(9)$	$X^+(^{10}B)/X^+(^{11}B)=2.112(18)$	[52]
	bb	$-2.212(11)$	$+2.091(8)$	$X^-(^{10}B)/X^-(^{11}B)=2.084(5)$	
	cc	$+3.896(11)$	$-2.186(8)$	$Q(^{10}B)/Q(^{11}B)=2.084(2)$	[15]
	Aminoborane, NH_2BH_2				
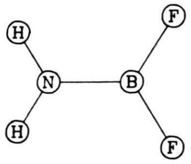	aa	$-1.971(6)$	$+0.890(5)$		[52]
	bb	$-0.500(11)$	$+2.303(7)$		
	cc	$+2.471(11)$	$-3.193(7)$		
	Aminodifluoroborane, NH_2BF_2				
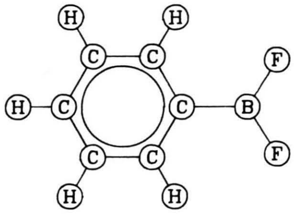	aa	$-2.589(12)$	–		[62]
	bb	$-0.600(15)$	–		
	cc	$+3.189(15)$	–		
	Phenyldifluoroborane, $C_6H_5BF_2$				

* absolute value, $\chi^+=-\chi_{aa}$, $\chi^-=\chi_{bb}-\chi_{cc}$.

by MW Stark spectroscopy. The increased sensitivity, resolution and precision of frequency determination is an important prerequisite.

In Table 1, results mainly for boron ^{11}B, with nuclear spin $I=3/2$ are given. For the first molecules the axes of the inertia and coupling tensor coincide. For BF_2OH with a plane of symmetry only the c inertia axis coincides with the y coupling tensor axis. By isotopic substitution and the resulting rotation of the molecule in the inertia axis system the principal coupling tensor axes can be calculated [57].

Figure 9 shows that the field gradient values of $q_{gg}=\partial^2 V/\partial g^2$ calculated with the program Gaussian [52, 58] using a 6-311 G** basis set can be correlated to the experimental values χ_{gg} by adjusting one parameter, an "effective" quadrupole moment, $Q=36.1$ mbarn. Also some boron coordination compounds were investigated [59–61].

Table 2 gives results for molecules containing iodine, I, with a nuclear spin $I=5/2$, and some other quadrupole nuclei like nitrogen, ^{14}N, and deuterium, D. Iodine is a strongly coupling nucleus.

Table 1 (continued)

	gg	$\chi_{gg}(^{11}B)$	gg	$\chi_{gg}(^{11}B)$	Ref.
	BF_2OH, Hydroxydifluoroborane				[52, 63]
	aa	$-1.447(5)$			
	bb	$-1.195(6)$			
	cc	$+2.672(6)$			
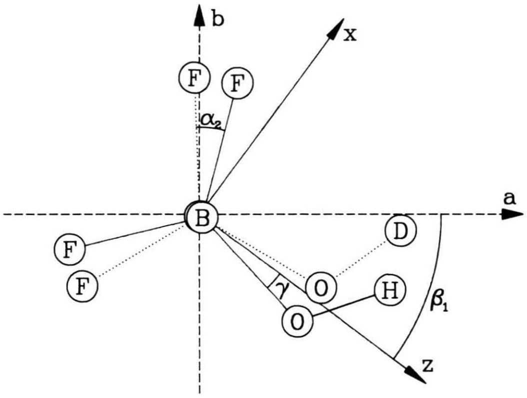	BF_2OD				
	aa	$-1.717(9)$			
	bb	$-0.960(9)$			
	cc	$+2.677(9)$			
	$BF_2{}^{18}OH$				
	aa	$-1.798(9)$	xx	$-0.857(8)$	
	bb	$-0.843(13)$	yy	$+2.672(6)$	
	cc	$+2.641(13)$	zz	$-1.816(8)$	
	$\alpha_2=16.676(149)°$, $\beta_1=36.72°$, $\gamma=10.75°$.				

Table 2. Iodine I, Spin $I=5/2$, $Q=-0.79$ barn [15].

	Y	gg	$\chi_{gg}(Y)$ [MHz]	gg	$C_{gg}(Y)$ [kHz]	Ref.
ICN	I	zz	$-2420.2228(13)$	xx	$10.55(5)$	[17]
	^{14}N	zz	$-4.0816(15)$	xx	$0.68(12)$	
$IC^{15}N$	I	zz	$-2419.9647(25)$	xx	$10.02(8)$	[64]
	^{15}N	zz	–	xx	$-1.51(49)$	
ICCH	I	zz	$-2254.284(15)$	xx	$9.5(5)$	[65]
$I^{13}CCH$	I	zz	$-2254.83(10)$			
$IC^{13}CH$	I	zz	$-2253.85(12)$			
ICCD	I	zz	$-2254.1785(34)$			
CH_3CH_2I	I	aa	$-1478.058(7)$	aa	$11.8(8)$	[66]
		bb	$564.413(5)$	bb	$7.5(2)$	
		cc	$913.644(5)$	cc	$9.5(2)$	
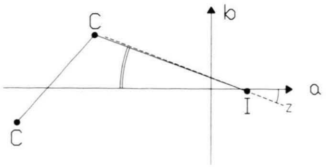		ab	$896.31(14)$			
		xx	$901.96(9)$			
		yy	$913.644(5)$			
		zz	$-1814.61(9)$			
		∢ (z, a)	$20.638(2)°$			
		∡ (a, CI)	$19.7°$	Structure see		[67]

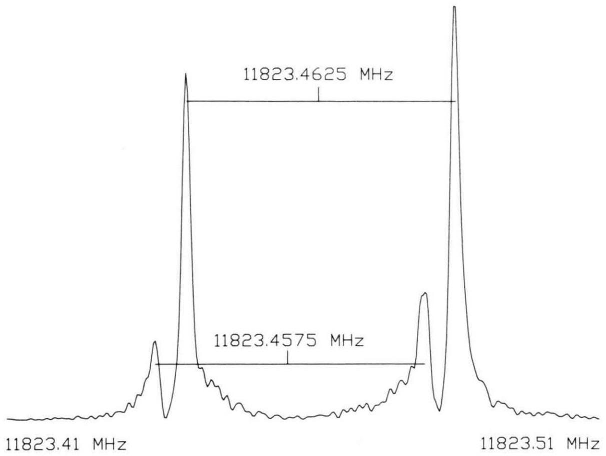

Fig. 8. 100 kHz section out of the recording of the J=1−0 transition of carbonyl sulfide, $O^{13}C^{34}S$, in natural abundance with ^{13}C spin-rotation hyperfine structure. Each line is split due to the Doppler effect by 45 kHz, the line width is 1 kHz (HWHH). Recording conditions: 100 ns sample interval, 8 K data points, extended with 24 k zeros prior to Fourier transformation, 1000 experiment cycles, 6 Hz experiment repetition rate [26].

In these measurements the precision of the frequency determination was important. Spin-rotation coupling had to be included in the analysis. As for I, off-diagonal elements $\chi_{gg'}$, $g \neq g'$, result from a precise analysis, the principal axis coupling tensor elements can be calculated easily by diagonalising the tensor.

The results for isopropyl iodide, CH_3CHICH_3, [68, 69] have not been included.

One observes a substantial change in the coupling constants. To my knowledge quantum chemistry is far from reproducing the experimental values.

In Table 3 I illustrate a quite different case, the coupling of deuterium, D, with nuclear spin 1. Here the coupling is extremely low. Only very few molecules [21] have been investigated before the advent of MWFT spectroscopy. Now the field is open especially with molecular beam MWFT spectroscopy.

For the first molecules in Table 3 the inertia and coupling tensor axes coincide. For these acetylenes the variation of χ_{zz} is quite small. For the following

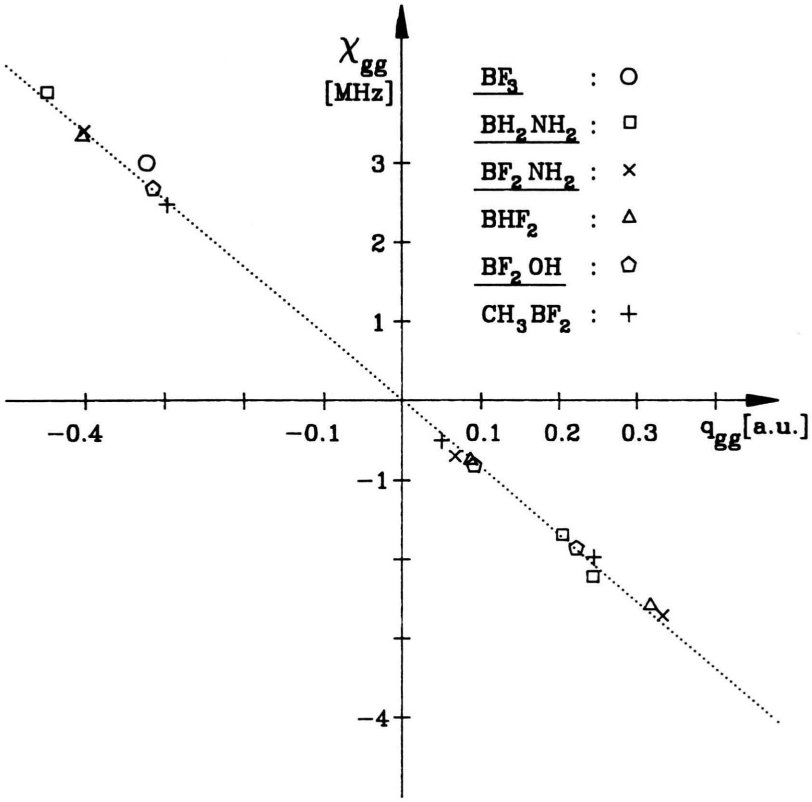

Fig. 9. Calculated field gradient q_{gg} correlated to coupling tensor elements χ_{gg} of a selection of boron compounds with trivalent boron. The nuclear quadrupole moment was adjusted to $Q = 36.1$ mbarn as single adjustable parameter. Program Gaussian 86 with basis set 6-311 G** [52].

Table 3. Deuterium D, Spin $I=1$, $Q=0.0028$ barn [15].

Substance	Y	gg	χ_{gg}(D) [kHz]	χ_{gg}(Y) [MHz]	C_I(Y) [kHz]	Ref.
$DC\equiv CF$		zz	205.4(12)	–	–	[71]
$DC\equiv C^{35}Cl$	^{35}Cl	zz	207.0(28)	−79.7358(19) *	1.10(31)	[72]
$DC\equiv C^{37}Cl$	^{37}Cl	zz	205.8(39)	−62.8451(27)	0.76(43)	
$DC\equiv C^{79}Br$	^{79}Br	zz	207.7(18)	+648.1381(21) **	6.40(18)	[71]
$DC\equiv C^{81}Br$	^{81}Br	zz	205.8(18) ***	+541.4454(20)	6.70(18)	
$DC\equiv CI$	I	zz	209.5(32)	−2254.1785(34)	8.55(19)	
$D{-}C\equiv C{-}C\equiv C{-}H$		zz	217(6)	–	–	[73]
DNCO	N	aa	57.6(54)	2.1237(15)	–	[74]
		bb	84.9(38)	−0.5528(18)	–	
		cc	−142.5(38)	−1.5709(18)	–	
		zz	285(6)	Assumption DN bond cyl. symmetric		
		(zz	286.3	calculated)		[70]
$D^{15}NO_3$		aa	31.1(24)	calculation		[75]
		bb	118.5(29)	see [75]		
		cc	−149.6(29)			

Deuterium D, Spin $I=1$, $Q = 0.0028$ barn [15]
Nitrogen N, Spin $I=1$, $Q = 0.02$ barn [15]

Substance	gg	χ_{gg}(D) [kHz]	χ_{gg}(N) [MHz]	Ref.	Substance	gg	χ_{gg}(D) [kHz]	χ_{gg}(N) [MHz]	Ref.
Piperidine	aa	−147(12)	−3.578(7)	[76]	Pyrrolidine	aa	−117(8)	−3.253(9)	[76]
$C_5H_{10}ND$	bb	−101(10)	2.806(5)		C_4H_8ND	bb	−94(11)	2.760(9)	[77]
	cc	+248(9)	0.772(8)		axial	cc	211(15)	0.493(17)	
	aa	–	−3.6763(11)			aa	–	−3.3904(14)	
axial	bb	–	2.8013(12)			bb	–	2.7642(14)	
	cc	–	0.8750(16)			cc	–	0.6262(20)	
	xx	–	1.74			xx	–	1.37	
	yy	–	2.8013(12)			yy	–	2.7642(14)	
	zz	–	−4.55			zz	–	−4.13	
equatorial	aa	232(9)	2.122(6)	[76]	Morpholine	aa	220(10)	2.166(6)	[78]
	bb	−117(9)	2.743(5)		OC_4H_8ND	bb	−108(6)	2.787(4)	
	cc	−115(15)	−4.865(7)		equatorial	cc	−112(11)	−4.953(6)	
	aa	–	2.1007(42)			aa	–	2.1491(24)	
	bb	–	2.7557(33)			bb	–	2.7966(25)	
	cc	–	−4.8564(39)			cc	–	−4.9457(24)	

* $\chi_{zz}(^{35}Cl)/\chi_{zz}(^{37}Cl) = 1.26877(8)$, $Q(^{35}Cl)/Q(^{37}Cl) = 1.26878(15)$ [15],
** $\chi_{zz}(^{79}Br)/\chi_{zz}(^{81}Br) = 1.197052(8)$. $Q(^{79}Br)/Q(^{81}Br) = 1.19707(3)$ [15].
*** The value of χ_{zz} in Table 4 of [71] is erroneus.

molecules, all containing a plane of symmetry, the determination of the principal coupling tensor elements is only possible by isotopic substitution [57] or by special assumptions, like a cylindersymmetric bond. Presently it is hopeless to determine off-diagonal elements of the coupling tensor. Resolution and precision are not adequate. But in the case of deuterium, Huber was successful to help by quantum chemical calculations with specially adapted basis sets describing the surroundings of D sufficiently [70].

Table 4 concludes the selection of examples with nitrogen compounds. Some nitrogen compounds were already given in the preceding tables. In those cases, spectra with multiple quadrupole coupling had to be analysed.

I chose isonitriles as example, as these generally ask for a high resolution. The first four molecules in Table 4 have coinciding inertia and coupling tensor axes. The remaining ones have a plane of symmetry. So only tensor components along an axis perpendic-

Table 4. Nitrogen ^{14}N, Spin $I=1$, $Q=0.02$ barn [15].

	gg	χ_{gg} [kHz]	C_{xx} [kHz]	Ref.
Isonitriles −NC				
CNCN	zz	+1318.5(78)	0.29	[8]
$(CH_3)_3CNC$	zz	+159.1(10)	–	[79]
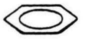 NC	aa bb cc	+411.5(70) −385.8(79) −25.7(79)	–	[79]
HC≡CNC	zz	945.4(8)	0.44(18)	[80]
$HC\equiv CCH_2NC$	aa bb cc	+290.3(78) +10.6(80) −300.9(80)	–	[81]
$CH_3CH_2CH_2NC$ gauche	aa bb cc	152(5) −9(7) −143(7)		[82]
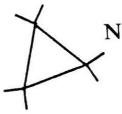 NC	aa bb cc	331(3) −128(9) −204(9)		[83]
$CH_2{=}CHNC$	aa bb cc	285(5) −258(6) 0(6)		[27]
CF_3NC	aa bb cc	1060(30) −530(15) −530(15)		[84]
CF_2HNC	aa bb cc	599(10) −406.5(14) −192.6(14)		[85]
CFH_2NC		–		
CH_3NC	aa bb cc	489.4(4) −244.7(2) −244.7(2)		[86]

ular to the symmetry plane can be compared without further assumption. Also here, isotopic substitution seems to be the only method to determine the coupling tensor principal axes. But there is not yet any example.

With elaborate quantum chemical calculations it is possible to reproduce the experimental data [87].

Interesting in the selection of Table 4 is the rather high value of χ_{zz} of $C^{14}NC^{15}N$.

We have investigated many molecules with nitrogen in different bond situations, like −CN, =N−, $-NH_2$, −N=O, $-NO_2$, −NCO, −NCS, −O−N=O, −NNN. Also the hfs of many heterocyclic ring compounds were analysed.

I think it was proved that MWFT spectroscopy revived the field of nuclear quadrupole coupling in molecular rotation spectra. Many problems are left to solve and many molecules wait for detailed investigation.

I thank my colleagues and coworkers for years of fruitful cooperation, especially Dr. W. Stahl for critically reading the manuscript. The funds were provided by the Deutsche Forschungsgemeinschaft, the Fonds der Chemie and the Land Schleswig-Holstein.

[1] W. Gordy and R. L. Cook, Microwave Molecular Spectra, 3rd ed., John Wiley and Sons, New York 1984.
[2] See [1], Chapter V.1.
[3] See [1], Chapter VI.
[4] See [1], Chapter VII.
[5] See [1], Chapter XIII.
[6] See [1], Chapter IX.
[7] See [1], Chapter IX.4, p. 407 f.
[8] M. C. L. Gerry, F. Stroh, and M. Winnewisser, J. Mol. Spectrosc. **140,** 147 (1990).
[9] See [1], Table 14.2. The value of Q for N has to be corrected to $Q=0.02$ barn.
[10] See [1], Chapter IX.5.
[11] See [1], Chapter XV.
[12] M. C. L. Gerry, N. Heineking, H. Mäder, and H. Dreizler, Z. Naturforsch. **44a,** 1079 (1989).
[13] N. Heineking and M. C. L. Gerry, Z. Naturforsch. **44a,** 669 (1989).
[14] See [1], Chapter IX.7.
[15] See [1], Appendix E.
[16] See [1], Eq. (9.151).
[17] J. Gripp and H. Dreizler, Z. Naturforsch. **43a,** 133 (1988).
[18] F. C. DeLucia and W. Gordy, Phys. Rev. **187,** 58 (1969) and [1], Table 9.5.
[19] R. H. Hughes and E. B. Wilson, jr., Phys. Rev. **71,** 562 L (1947).
[20] C. H. Townes and A. L. Schawlow, Microwave Spectroscopy, McGraw Hill, New York 1955, Chapter 15.
[21] Landolt-Börnstein, Numerical Data and Functional Relationships in Science and Technology, Vol. II/14, II/6, II/4, Springer, Berlin 1982, 1974, 1967. – J. Vogt, Structural Chemical Database for Gas Phase Compounds. Structural Chemistry, 1992 in press.
[22] J. Ekkers and W. H. Flygare, Rev. Sci. Instrum. **47,** 448 (1976).
[23] T. J. Balle and W. H. Flygare, Rev. Sci. Instrum. **52,** 1 (1981).
[24] G. Bestmann, H. Dreizler, H. Mäder, and U. Andresen, Z. Naturforsch. **35a,** 392 (1980).
[25] U. Andresen, H. Dreizler, J.-U. Grabow, and W. Stahl, Rev. Sci. Instrum. **61,** 3694 (1990).
[26] J. U. Grabow and W. Stahl, Z. Naturforsch. **45a,** 1043 (1990).
[27] G. Bestmann and H. Dreizler, Z. Naturforsch. **37a,** 58 (1982).
[28] G. Bestmann and H. Dreizler, Z. Naturforsch. **37a,** 615 (1982).
[29] H. Dreizler, E. Fliege, H. Mäder, and W. Stahl, Z. Naturforsch. **37a,** 1266 (1982).

[30] G. Bestmann, H. Dreizler, E. Fliege, and W. Stahl, J. Mol. Struct. **97,** 215 (1983).
[31] G. Bestmann and H. Dreizler, Z. Naturforsch. **38a,** 452 (1983).
[32] W. Stahl, E. Fliege, H. Dreizler, and R. Schwarz, Z. Naturforsch. **38a,** 354 (1984).
[33] W. Stahl, E. Fliege, and H. Dreizler, Z. Naturforsch. **39a,** 858 (1984).
[34] W. Stahl, G. Bestmann, H. Dreizler, U. Andresen, and R. Schwarz, Rev. Sci. Instrum. **56,** 1759 (1985).
[35] E. Fliege and H. Dreizler, Z. Naturforsch. **42a,** 72 (1987).
[36] W. Stahl, J. Gripp, N. Heineking, and H. Dreizler, Z. Naturforsch. **42a,** 392 (1987).
[37] H. Dreizler, U. Andresen, J. Gripp, I. Merke, M. Meyer, W. Stahl, R. Schwarz, and K. Vormann, Z. Naturforsch. **42a,** 1279 (1987).
[38] N. Heineking, W. Stahl, and H. Dreizler, Z. Naturforsch. **43a,** 280 (1988).
[39] P. Wolf and H. Mäder, Mol. Phys. **64,** 43 (1988).
[40] U. Andresen and B. Kleibömer, Rev. Sci. Instrum. **59,** 1088 (1988).
[41] Ch. Keussen, N. Heineking, and H. Dreizler, Z. Naturforsch. **44a,** 215 (1989).
[42] H. Ehrlichmann, J.-U. Grabow, H. Dreizler, N. Heineking, R. Schwarz, and U. Andresen, Z. Naturforsch. **44a,** 751 (1989).
[43] Ch. Keussen, R. Schwarz, U. Andresen, and H. Dreizler, Z. Naturforsch. **45a,** 711 (1990).
[44] M. Krüger and H. Dreizler, Z. Naturforsch. **45a,** 724 (1990).
[45] H. S. Gutowsky, C. Chuang, T. D. Klotz, T. Emilsson, R. S. Ruoff, and K. R. Krause, J. Chem. Phys. **88,** 2919 (1988).
[46] M. Oldani, M. Andrist, A. Bauder, and A. G. Robiette, J. Mol. Spectrosc. **110,** 93 (1985).
[47] P. Wolf and W. Stahl, Z. Naturforsch. **44a,** 651 (1989).
[48] W. Stahl, H. Dreizler, L. Jörissen, and W. A. Kreiner, Z. Naturforsch. **41a,** 747 (1986).
[49] W. Stahl and H. Dreizler, Z. Naturforsch. **42a,** 1402 (1987).
[50] G. Bestmann, W. Lalowski, and H. Dreizler, Z. Naturforsch. **40a,** 271 (1985).
[51] M. Oldani and A. Bauder, J. Chem. Phys. **86,** 624 (1987).
[52] Kirsten Vormann, Dissertation, Kiel 1991; K. Vormann, H. Dreizler, J. Doose, and A. Guarnieri, Z. Naturforsch. **46a,** 770 (1991); K. Vormann and H. Dreizler, Z. Naturforsch. **46,** 909 (1991).
[53] I. Merke and H. Dreizler, Z. Naturforsch. **43a,** 196 (1988).
[54] J. Haekel and H. Mäder, Z. Naturforsch. **43a,** 203 (1988).
[55] H. Dreizler, Molecular Physics **59,** 1 (1986).
[56] J. C. McGurk, T. G. Schmalz, and W. H. Flygare, Adv. Chem. Phys. **25,** 1 (1974).
[57] See [1], Chapter IX.4, p. 418f.
[58] Gaussian 86, M. J. Frisch, J. S. Brinkley, H. B. Schlegel, K. Raghavachari, C. F. Melius, R. L. Martin, J. J. P. Stewart, F. W. Bobrowicz, C. M. Rohlfing, L. R. Kahn, D. J. Defrees, R. Seeger, R. A. Whiteside, D. J. Fox, E. M. Fleuder, and J. A. Pople, Carnegie-Mellon Quantum Chemistry Publishing Unit, Pittsburg PA, 1984.
[59] W. Kasten, H. Dreizler, and R. L. Kuczkowski, Z. Naturforsch. **40a,** 1262 (1985).
[60] W. Karsten, H. Dreizler, and R. L. Kuczkowski, Z. Naturforsch. **40a,** 920 (1985).
[61] W. Kasten, H. Dreizler, R. L. Kuczkowski, and M. S. LaBarge, Z. Naturforsch. **41a,** 835 (1986).
[62] Kirsten Vormann and H. Dreizler, Z. Naturforsch. **44a,** 84 (1989).
[63] Kirsten Vormann and H. Dreizler, Z. Naturforsch. **44a,** 1191 (1989).
[64] J. Gripp, H. Dreizler, J. Gadhi, G. Wlodarczak, J. Lebrand, J. Burie, and J. Demaison, J. Mol. Spectrosc. **129,** 381 (1988).
[65] U. Andresen, N. Heineking, and H. Dreizler, J. Mol. Spectrosc. **137,** 296 (1989).
[66] J. Gripp and H. Dreizler, Z. Naturforsch. **43a,** 971 (1988).
[67] T. Inagusa, M. Fujitake, and M. Hayashi, J. Mol. Spectrosc. **128,** 456 (1988).
[68] J. Gripp and H. Dreizler, Z. Naturforsch. **345a,** 715 (1990).
[69] C. Ikeda, T. Inagusa, and M. Hayashi, J. Mol. Spectrosc. **135,** 334 (1989).
[70] H. Huber, J. Chem. Phys. **83,** 4591 (1985).
[71] N. Heineking, M. Andolfatto, C. Kruse, W. Eberstein, and H. Dreizler, Z. Naturforsch. **43a,** 755 (1988).
[72] N. Heineking, M. Andolfatto, U. Keussen, A. Mues, and H. Dreizler, Z. Naturforsch. **44a,** 735 (1989).
[73] O. Böttcher, N. Heineking, M. Andolfatto, and D. H. Sutter, Z. Naturforsch. **44a,** 89 (1989).
[74] N. Heineking, M. C. L. Gerry, and H. Dreizler, Z. Naturforsch. **44a,** 577 (1989).
[75] E. Fliege, H. Dreizler, S. Gerber, and H. Huber, J. Mol. Spectrosc. **137,** 24 (1989).
[76] H. Ehrlichmann, J. U. Grabow, H. Dreizler, N. Heineking, and M. Andolfatto, Z. Naturforsch. **44a,** 841 (1989).
[77] H. Ehrlichmann, J. U. Grabow, and H. Dreizler, Z. Naturforsch. **44a,** 837 (1989).
[78] J. U. Grabow, H. Ehrlichmann, and H. Dreizler, Z. Naturforsch. **44a,** 833 (1989).
[79] W. Kasten, H. Dreizler, and U. Andresen, Z. Naturforsch. **41a,** 1302 (1986).
[80] M. Krüger, H. Dreizler, D. Preugschat, and D. Lentz, Angew. Chem. **103,** 1674 (1991); Angew. Chem. Int. Ed. Engl. **30,** 1645 (1991).
[81] M. Krüger and H. Dreizler, Z. Naturforsch. **45a,** 986 (1990).
[82] K. Vormann, R. Schwarz, and H. Dreizler, Z. Naturforsch. **43a,** 277 (1988).
[83] E. Fliege, H. Dreizler, and R. Schwarz, J. Mol. Struct. **97,** 229 (1983).
[84] D. Christen, K. Ramme, B. Haas, H. Oberhammer, and D. Lentz, J. Chem. Phys. **80,** 4020 (1984).
[85] M. Krüger, to be published.
[86] S. G. Kukolich, J. Chem. Phys. **57,** 869 (1972).
[87] D. Cremer and M. Krüger, J. Phys. Chem. 1992 in press.